

EPJ Web of Conferences 5, 05017 (2010)

DOI:10.1051/epjconf/20102505017

© Owned by the authors, published by EDP Sciences, 2010

Approximate Three-Dimensional Wave Function and the T-Matrix for the Sharply Cut Off Coulomb Potential

J. Golak^{1,a}, W. Glöckle², R. Skibiński¹, and H. Witała¹¹ M. Smoluchowski Institute of Physics, Jagiellonian University, PL-30059 Kraków, Poland² Institut für theoretische Physik II, Ruhr-Universität Bochum, D-44780 Bochum, Germany

Abstract. For a sharply cut-off Coulomb potential we derive analytically the asymptotic form of the three-dimensional wave function and the related scattering amplitude. We show a failure of the standard renormalization factor which is believed to be generally valid for any type of screening. We obtain also the asymptotic form of the corresponding three-dimensional half-shell t-matrix. Our results are fully supported by the numerical solutions of the three-dimensional Lippmann-Schwinger equation.

1 Introduction

The long range behavior of the Coulomb force causes technical problems in the scattering for more than two particles. A possible solution proposed long time ago is to start with a screened Coulomb potential. In the limit of an infinite screening radius it is claimed in the literature [1–3] that the on-shell two-body t-matrix approaches the physical one except for an infinitely oscillating phase factor, known analytically. By removing that factor (the so-called renormalization) the physical result can be obtained. As a basis for that approach papers by Gorshkov [4,5], Ford [6,7] and Taylor [1,2] are most often quoted. However, only Gorshkov [4,5] works directly in three dimensions and other authors rely on a partial wave decomposition. This leaves at least doubts about the rigorousness of that approach, where the infinite sum over angular momenta is carried out without control of its validity for the correction terms.

In such a situation we felt that a rigorous analytical approach for a sharply cut off Coulomb potential carried through directly in three dimensions is in order. This presentation based on our two papers [8,9] delivers the asymptotic form of the three-dimensional wave function (section 2) and the scattering amplitude (section 3). We obtain also the asymptotic form of the corresponding three-dimensional half-shell t-matrix (section 4). These purely analytical results are confirmed by numerical studies presented in section 5. We summarise in section 6.

^a e-mail: jacek.golak@uj.edu.pl

2 The wave function for a sharply cut-off Coulomb potential

Let us regard two equally charged particles with mass m . Then the two-body Schrödinger equation reads

$$(-\nabla^2 - p^2 + \frac{me^2}{r})\Psi^{(+)}(\mathbf{r}) = 0. \quad (1)$$

It is well known that in the parabolic coordinates

$$\begin{aligned} u &= r - z \\ v &= r + z \\ \cos \phi &= x/r, \quad \sin \phi = y/r, \end{aligned} \quad (2)$$

the partial differential equation factorizes and yields the solution

$$\Psi^{(+)}(\mathbf{r}) = \text{const } e^{i\mathbf{p}\cdot\mathbf{r}} {}_1F_1(-i\eta, 1, i(pr - \mathbf{p}\cdot\mathbf{r})) \quad (3)$$

with Sommerfeld parameter $\eta = \frac{me^2}{2p}$.

Now we switch to a sharply screened Coulomb potential

$$V(r) = \Theta(R - r) \frac{e^2}{r} \quad (4)$$

and rewrite (1) into the form of the Lippmann-Schwinger equation

$$\begin{aligned} \Psi_R^{(+)}(\mathbf{r}) &= \frac{1}{(2\pi)^{3/2}} e^{i\mathbf{p}\cdot\mathbf{r}} \\ &- \frac{m}{4\pi} \int d^3r' \frac{e^{i\mathbf{p}\cdot(\mathbf{r}-\mathbf{r}')}}{|\mathbf{r}-\mathbf{r}'|} \Theta(R - r') \frac{e^2}{r'} \Psi_R^{(+)}(\mathbf{r}'). \end{aligned} \quad (5)$$

This defines uniquely the wave function $\Psi_R^{(+)}(\mathbf{r})$ for a given cut-off radius R . For $r < R$ we assume that

$$\Psi_R^{(+)}(\mathbf{r}) = A e^{i\mathbf{p}\cdot\mathbf{r}} {}_1F_1(-i\eta, 1, i(pr - \mathbf{p}\cdot\mathbf{r})) \quad (6)$$

with some to be found constant A . (As pointed out in [10] this assumption is not generally correct and valid only in the limit of the infinite cut-off radius.) Next we insert this form (6) into the Lippmann-Schwinger equation (5) obtaining for $r < R$ the following identity

$$Ae^{i\mathbf{p}\cdot\mathbf{r}} {}_1F_1(-i\eta, 1, i(pr - \mathbf{p}\cdot\mathbf{r})) = \frac{1}{(2\pi)^{3/2}} e^{i\mathbf{p}\cdot\mathbf{r}} - \frac{m}{4\pi} \int d^3r' \frac{e^{i\mathbf{p}|\mathbf{r}-\mathbf{r}'|}}{|\mathbf{r}-\mathbf{r}'|} \Theta(R-r') \frac{e^2}{r'} \times A e^{i\mathbf{p}\cdot\mathbf{r}'} {}_1F_1(-i\eta, 1, i(pr' - \mathbf{p}\cdot\mathbf{r}')), \quad (7)$$

which determines the factor A . We choose $\hat{\mathbf{p}} = \hat{\mathbf{z}}$ and work with the parabolic coordinates. Then (7) turns into

$$Ae^{i\frac{p}{2}(v-u)} {}_1F_1(-i\eta, 1, ipu) = \frac{1}{(2\pi)^{3/2}} e^{i\frac{p}{2}(v-u)} + A \frac{e^2}{2} \int_0^{2R} du' e^{-i\frac{p}{2}u'} {}_1F_1(-i\eta, 1, ipu') \times \int_0^{2R-u'} dv' e^{i\frac{p}{2}v'} \left(-\frac{m}{4\pi}\right) \int_0^{2\pi} d\phi' \frac{e^{i\mathbf{p}|\mathbf{r}-\mathbf{r}'|}}{|\mathbf{r}-\mathbf{r}'|}. \quad (8)$$

Since we want to determine just one factor A one value of u and v is sufficient and we choose the simplest case $u = v = 0$. Then the ϕ' integration is trivial and one obtains

$$A = \frac{1}{(2\pi)^{3/2}} - A \frac{e^2 m}{2} \int_0^{2R} du' {}_1F_1(-i\eta, 1, ipu') \times \int_0^{2R-u'} dv' e^{ipv'} \frac{1}{u' + v'}, \quad (9)$$

where we used ${}_1F_1(-i\eta, 1, 0) = 1$. Substituting $u' = 2Rx$, $v' = 2Ry$ and defining $A \equiv \tilde{A} \frac{1}{(2\pi)^{3/2}}$ one obtains

$$\tilde{A} = 1 - \tilde{A}\eta T \int_0^1 dx {}_1F_1(-i\eta, 1, iTx) \int_0^{1-x} dy e^{iTy} \frac{1}{x+y} \quad (10)$$

with $T \equiv 2pR$.

Introducing $z \equiv iT$ let us define

$$\tilde{F}(z) = 1 + \frac{\eta z}{i} \int_0^1 dx {}_1F_1(-i\eta, 1, zx) \int_0^{1-x} dy e^{zy} \frac{1}{x+y}. \quad (11)$$

Substituting $zx = \tau$, $zy = \tau'$ we get

$$\tilde{F}(z) = 1 - i\eta \int_0^z d\tau {}_1F_1(-i\eta, 1, \tau) \int_0^{z-\tau} d\tau' e^{\tau'} \frac{1}{\tau + \tau'}. \quad (12)$$

Then it follows

$$\begin{aligned} \frac{d\tilde{F}(z)}{dz} &= -\frac{i\eta}{z} e^z \int_0^z d\tau {}_1F_1(-i\eta, 1, \tau) e^{-\tau} \quad (13) \\ \frac{d^2\tilde{F}(z)}{dz^2} &= \frac{i\eta}{z^2} e^z \int_0^z d\tau {}_1F_1(-i\eta, 1, \tau) e^{-\tau} - \frac{i\eta}{z} e^z \int_0^z d\tau {}_1F_1(-i\eta, 1, \tau) e^{-\tau} \\ &\quad - \frac{i\eta}{z} e^z \int_0^z d\tau {}_1F_1(-i\eta, 1, \tau) e^{-\tau} \\ &= -\frac{1}{z} \frac{d\tilde{F}(z)}{dz} + \frac{d\tilde{F}(z)}{dz} - \frac{i\eta}{z} {}_1F_1(-i\eta, 1, z). \quad (14) \end{aligned}$$

Consequently

$$z \frac{d^2\tilde{F}(z)}{dz^2} + (1-z) \frac{d\tilde{F}(z)}{dz} = -i\eta {}_1F_1(-i\eta, 1, z). \quad (15)$$

We add $i\eta\tilde{F}(z)$ on both sides

$$\begin{aligned} z \frac{d^2\tilde{F}(z)}{dz^2} + (1-z) \frac{d\tilde{F}(z)}{dz} + i\eta\tilde{F}(z) \\ = i\eta(\tilde{F}(z) - {}_1F_1(-i\eta, 1, z)). \quad (16) \end{aligned}$$

The left side put to zero is the defining differential equation for ${}_1F_1(-i\eta, 1, z)$. Thus (16) is fulfilled for

$$\tilde{F}(z) = {}_1F_1(-i\eta, 1, z) \quad (17)$$

which also fixes the normalisation. We end up with the exact formula for \tilde{A}

$$\tilde{A} = \frac{1}{{}_1F_1(-i\eta, 1, iT)}. \quad (18)$$

and the asymptotic form of the wave function for $r < R$

$$\psi_R^{(+)}(\mathbf{r}) = \frac{1}{(2\pi)^{3/2}} \frac{1}{{}_1F_1(-i\eta, 1, iT)} e^{i\mathbf{p}\cdot\mathbf{r}} {}_1F_1(-i\eta, 1, i(pr - \mathbf{p}\cdot\mathbf{r})). \quad (19)$$

3 The scattering amplitude

The scattering amplitude f_R is defined for $r \rightarrow \infty$ by

$$\psi_R^{(+)}(\mathbf{r}) \rightarrow \frac{1}{(2\pi)^{3/2}} e^{i\mathbf{p}\cdot\mathbf{r}} + \frac{e^{ipr}}{r} f_R. \quad (20)$$

Using (5) and (19), our starting point becomes

$$\begin{aligned} \tilde{f}_R &= \tilde{A} \left(-\frac{m}{4\pi}\right) \int_{r' < R} d^3r' e^{-i\mathbf{p}\hat{\mathbf{r}}\cdot\mathbf{r}'} \frac{e^2}{r'} e^{i\mathbf{p}\cdot\mathbf{r}'} \\ &\quad \times {}_1F_1(-i\eta, 1, (pr' - \mathbf{p}\cdot\mathbf{r}')). \quad (21) \end{aligned}$$

where $\tilde{f}_R = \frac{1}{(2\pi)^{3/2}} f_R$. We use the general integral representation of ${}_1F_1(\alpha, \beta, z)$

$${}_1F_1(\alpha, \beta, z) = C(\alpha, \beta) \int_{\Gamma} dt e^{zt} t^{\alpha-1} (1-t)^{\beta-\alpha-1} \quad (22)$$

where the path Γ encircles the logarithmic cut between $t = 0$ and $t = 1$ in the positive sense and the prefactor is

$$C(\alpha, \beta) = \frac{\Gamma(\beta)}{\Gamma(\alpha)\Gamma(\beta-\alpha)} \frac{1}{1 - e^{2\pi i(\beta-\alpha)}}. \quad (23)$$

After lengthy algebra [8] we obtain

$$\begin{aligned} \tilde{f}_R &= (2\tilde{R})^{-2i\eta} A_c(\theta) + \\ &\quad \frac{\eta}{4p \sin^2 \frac{\theta}{2}} \left[e^{2i\tilde{R} \sin \frac{\theta}{2}} \left(\frac{1 - \sin \frac{\theta}{2}}{2} \right)^{i\eta} \right. \end{aligned}$$

$$\begin{aligned}
 & + e^{-2i\tilde{R} \sin \frac{\theta}{2}} \left(\frac{1 + \sin \frac{\theta}{2}}{2} \right)^{i\eta} \Bigg] \\
 & = \left[e^{-2i\eta \ln(2\tilde{R})} - \right. \\
 & \left. \frac{1}{2} e^{i\eta \ln \sin^2 \frac{\theta}{2} - 2i\sigma_0} \left(e^{2i\tilde{R} \sin \frac{\theta}{2} + i\eta \ln \frac{1 - \sin \frac{\theta}{2}}{2}} + \right. \right. \\
 & \left. \left. e^{-2i\tilde{R} \sin \frac{\theta}{2} + i\eta \ln \frac{1 + \sin \frac{\theta}{2}}{2}} \right) \right] A_c(\theta), \quad (24)
 \end{aligned}$$

where the physical Coulomb scattering amplitude is

$$A_c(\theta) = -\frac{\eta}{2p} \frac{(\sin^2 \frac{\theta}{2})^{-i\eta}}{\sin^2 \frac{\theta}{2}} e^{2i\sigma_0}, \quad (25)$$

$$\frac{\Gamma(1+i\eta)}{\Gamma(1-i\eta)} \equiv e^{2i\sigma_0} \quad (26)$$

and θ is the scattering angle.

Only the first term in (24) is the result expected from the literature, see [1, 3] and references therein. This means that the derivations based on partial wave decomposition must be incomplete.

4 Half-shell t-matrix

The asymptotic form of the half-shell t-matrix is given as

$$\begin{aligned}
 \langle \mathbf{p}' | V_R | \Psi_R^{(+)} \rangle & = \frac{1}{(2\pi)^{3/2}} A \int d^3 r e^{-i\mathbf{p}' \cdot \mathbf{r}} V_R(r) e^{i\mathbf{p} \cdot \mathbf{r}} \\
 & \times {}_1F_1(-i\eta, 1, i(pr - \mathbf{p} \cdot \mathbf{r})). \quad (27)
 \end{aligned}$$

As before, we start from the integral representation of the confluent hypergeometric function

$$\begin{aligned}
 & {}_1F_1(-i\eta, 1, i(pr - \mathbf{p} \cdot \mathbf{r})) = \\
 & C(-i\eta, 1) \int_{\Gamma} dt \left(\frac{1-t}{t} \right)^{i\eta} \frac{1}{t} e^{i(pr - \mathbf{p} \cdot \mathbf{r})t}. \quad (28)
 \end{aligned}$$

The r -integral is straightforward leading to

$$\begin{aligned}
 & \int_{r < R} d^3 r e^{i(\mathbf{p} - \mathbf{p}') \cdot \mathbf{r}} \frac{1}{r} e^{iprt} e^{-i\mathbf{p} \cdot \mathbf{r}} = \\
 & \frac{-4\pi}{2\Omega} \left[\frac{e^{i(pt + \Omega)R} - 1}{pt + \Omega} - \frac{e^{i(pt - \Omega)R} - 1}{pt - \Omega} \right] \quad (29)
 \end{aligned}$$

with

$$\Omega = \sqrt{p^2 t^2 - 2t\mathbf{p} \cdot \mathbf{\Delta} + \Delta^2}, \quad (30)$$

$$\mathbf{\Delta} = \mathbf{p} - \mathbf{p}'. \quad (31)$$

Thus

$$\langle \mathbf{p}' | V_R | \Psi_R^{(+)} \rangle \equiv -2\pi \frac{e^2}{(2\pi)^{3/2}} AC(-i\eta, 1) Y, \quad (32)$$

where

$$Y = \int_{\Gamma} dt \left(\frac{1-t}{t} \right)^{i\eta} \frac{1}{t} \frac{1}{\Omega} \left[\frac{e^{i(pt + \Omega)R} - 1}{pt + \Omega} - \frac{e^{i(pt - \Omega)R} - 1}{pt - \Omega} \right] \quad (33)$$

Next we have to distinguish the two cases: $p' > p$ and $p' < p$. After complicated algebra [9] we obtain for $p' < p$ the following result in the screening limit

$$\begin{aligned}
 \langle \mathbf{p}' | V_R | \Psi_R^{(+)} \rangle & \rightarrow e^{-i\eta \ln 2pR} \langle \mathbf{p}' | V_C | \Psi_{\mathbf{p}}^{C(+)} \rangle \\
 & - \frac{e^2}{(2\pi)^2} \frac{1}{\Delta^2} \left[e^{iR\Delta} \left(\frac{1}{2} (p - \frac{\mathbf{p} \cdot \mathbf{\Delta}}{\Delta}) \right)^{i\eta} + \right. \\
 & \left. e^{-iR\Delta} \left(\frac{1}{2} (p + \frac{\mathbf{p} \cdot \mathbf{\Delta}}{\Delta}) \right)^{i\eta} \right], \quad (34)
 \end{aligned}$$

the pure half shell t-matrix is well known [11] and for $p' < p$ given by

$$\langle \mathbf{p}' | V_C | \Psi_{\mathbf{p}}^{C(+)} \rangle = \frac{e^2}{2\pi^2} e^{\frac{\pi}{2}\eta} \Gamma(1+i\eta) \frac{1}{\Delta^2} \left(\frac{p^2 - p'^2}{\Delta^2} \right)^{i\eta} \quad (35)$$

The first term in (34) is expected [6]. But there is, like for the on-shell t-matrix, an additional term, which only after integration over some angular region would disappear in the screening limit.

In the case of $p' > p$ the pure half shell t-matrix differs by a factor $e^{-\pi\eta}$ and is

$$\langle \mathbf{p}' | V_C | \Psi_{\mathbf{p}}^{C(+)} \rangle = \frac{e^2}{2\pi^2} e^{-\frac{\pi}{2}\eta} \Gamma(1+i\eta) \frac{1}{\Delta^2} \left(\frac{p'^2 - p^2}{\Delta^2} \right)^{i\eta} \quad (36)$$

In this case we find the following result in the screening limit

$$\begin{aligned}
 \langle \mathbf{p}' | V_R | \Psi_R^{(+)} \rangle & \rightarrow e^{-i\eta \ln 2pR} \langle \mathbf{p}' | V_C | \Psi_{\mathbf{p}}^{C(+)} \rangle \\
 & - e^{2\pi\eta} \frac{e^2}{(2\pi)^2} \frac{1}{\Delta^2} \left[e^{iR\Delta} \left(\frac{1}{2} (p - \frac{\mathbf{p} \cdot \mathbf{\Delta}}{\Delta}) \right)^{i\eta} + \right. \\
 & \left. e^{-iR\Delta} \left(\frac{1}{2} (p + \frac{\mathbf{p} \cdot \mathbf{\Delta}}{\Delta}) \right)^{i\eta} \right]. \quad (37)
 \end{aligned}$$

The first term has the same structure as in (34) but the second one differs by the factor $e^{2\pi\eta}$ from the one in (34).

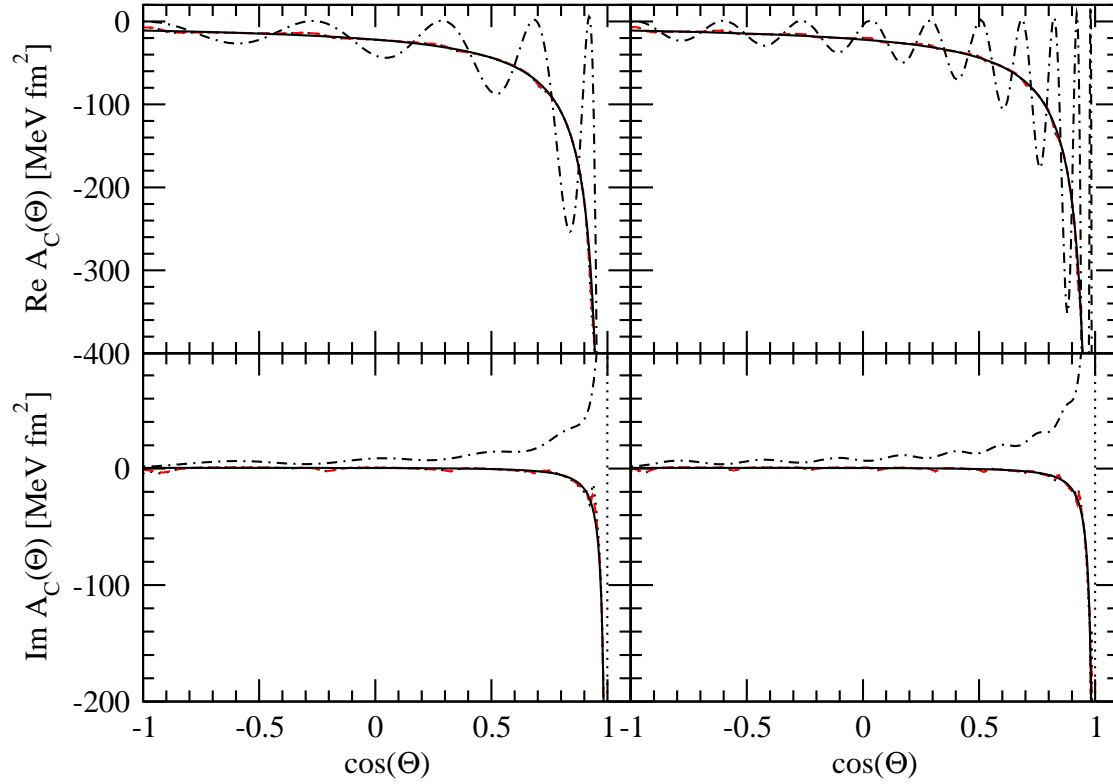
5 Numerical results

We performed a number of numerical tests to check the basic points of our algebra leading to the asymptotic form of the wave function and the scattering amplitude [8]. For example we calculated the relative difference between left and right sides of Eq. (8) for a number of points inside the region $r < R$. The results are shown in Table 1.

To check the quality of our renormalization factor (24) we applied it directly to the numerical solutions of the Lippmann-Schwinger equation obtained in the momentum space for the sharply cut off Coulomb potential. Details of the numerical performance can be found in [12, 8]. In Fig. 1 we compare the resulting transition amplitudes $A_C(\theta) \equiv -2\pi^2 m T(q_0, q_0, \cos \theta)$ with the pure Coulomb amplitude for $R = 40$ and 80 fm. With increasing cut-off radius a development of strong oscillations in the scattering angle dependence for the real parts of the numerical solutions is clearly seen. These oscillations follow on average the real part of the pure Coulomb amplitude given

Table 1. The relative difference between left (L13) and right (R13) sides of Eq. (8): $\frac{|L13-R13|}{|R13|} \times 100\%$ for different directions of \mathbf{r} at $E=3$ and $E=13$ MeV.

R [fm]	r [fm]	E=3 MeV			E=13 MeV		
		$\theta = 30^\circ$	$\theta = 90^\circ$	$\theta = 150^\circ$	$\theta = 30^\circ$	$\theta = 90^\circ$	$\theta = 150^\circ$
100	80	1.83487	2.37415	0.54698	0.41693	1.03684	0.19990
150	80	0.29032	0.82779	0.30193	0.11503	0.38629	0.10682
200	80	0.42749	0.35520	0.20520	0.07251	0.15571	0.03989
500	80	0.02969	0.08112	0.06497	0.02827	0.02510	0.00620
1000	80	0.01216	0.02270	0.03268	0.01309	0.01621	0.00347

**Fig. 1.** (Color online) The real (top) and imaginary (bottom) part of $A_C(\theta) \equiv -2\pi^2 m T(q_0, q_0, \cos \theta)$ as a function of $\cos \theta$ for $R=40$ fm (left panel) and 80 fm (right panel) at $E_p^{lab} = 13$ MeV. The dash-dotted line represents a direct numerical prediction (without any renormalization). The dotted line shows $A_C(\theta)$ with inclusion of the asymptotic renormalization factor given in (24) and the dashed (red) line is for $A_C(\theta)$ with inclusion of a more general renormalization factor [8]. The solid line represents the pure Coulomb amplitude given in (25).

by (25) and shown by the solid line. The imaginary parts of the numerical solutions are totally off from the imaginary part of the pure Coulomb amplitude and have even an opposite sign. Applying to the numerical solutions the asymptotic renormalization factor from (24) dramatically improves the agreement. Not only the oscillations in the real parts are removed and the pure Coulomb and renormalised amplitudes are practically overlapping but the renormalization brings also imaginary parts into agreement with the exception of very forward angles. We also checked that the two additional terms in the renormalization factor of (24) are absolutely crucial and that the “standard” renormalization (without these terms) fails totally. This is demonstrated in Fig. 2.

In Fig. 3 we compare the derived asymptotic form of the half-shell t-matrix, $T(q', q_0, x; q_0)$, with the correspond-

ing numerical solutions of the Lippmann-Schwinger equation for the screening radius $R=80$ fm. The analytical asymptotic form agrees rather well with the numerical result for the real part. The agreement is in fact very good in the region of $q' < q_0$ and a bit less satisfactory for $q' > q_0$. For the imaginary part there are clear deviations between the analytical and numerical results, which become more pronounced for $x \geq 0$. In particular the analytical results show much more oscillatory behavior for $q' > q_0$. Note also a sharp structure around $q' = q_0$ which develops for the imaginary part at $x \geq 0$.

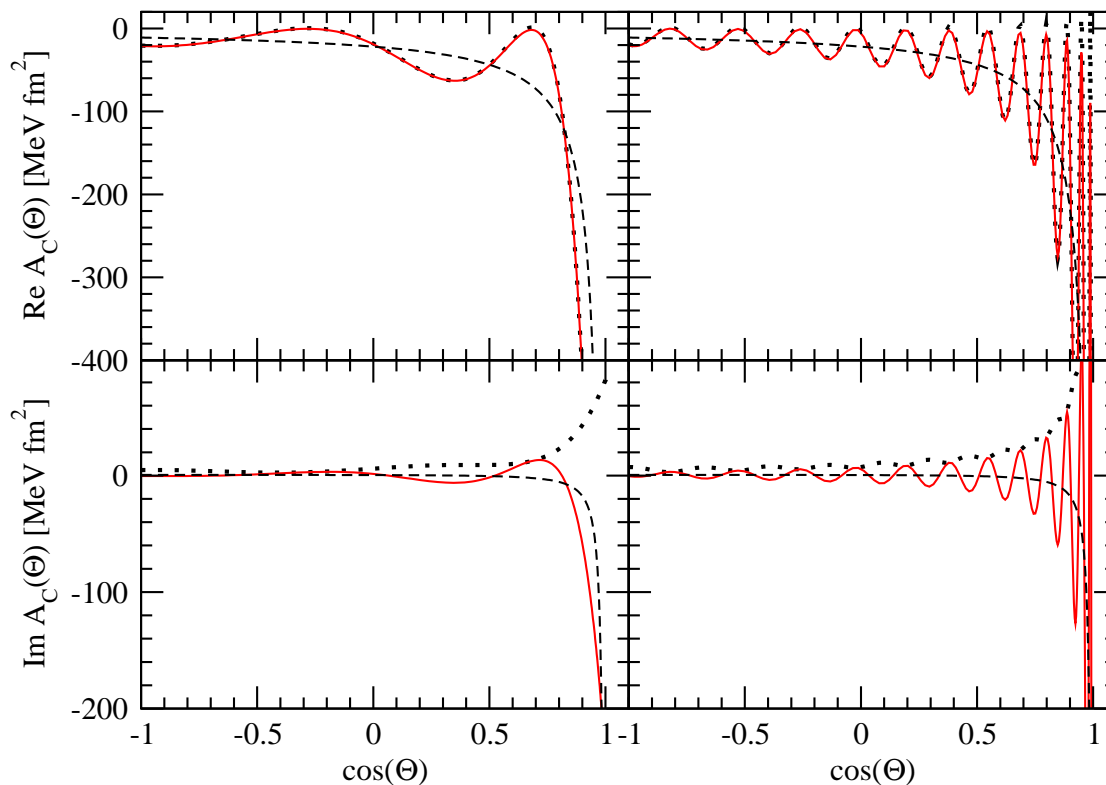


Fig. 2. (Color online) The real (top) and imaginary (bottom) part of $A_C(\theta) \equiv -2\pi^2 m T(q_0, q_0, \cos \theta)$ as a function of $\cos \theta$ for $R=20$ fm (left panel) and 100 fm (right panel) at $E_p^{lab} = 13$ MeV. The dotted line represents a direct numerical prediction (without any renormalization). The solid (red) line shows $A_C(\theta)$ with renormalization factor $e^{-2i\eta \ln(2pR)}$ and the dashed line represents the pure Coulomb amplitude given in (25).

6 Summary

The renormalization method for a screened on-shell Coulomb t-matrix enjoys a widespread use; see for instance [13,14]. As pointed out in the introduction the underlying mathematical considerations leave room for doubts. To shed light on that issue we regarded potential scattering on the sharply cut-off Coulomb potential directly in three dimensions, avoiding difficulties in the infinite sum of angular momenta. We succeeded to determine analytically the asymptotic form of the wave function. This allowed us to derive the analytical expression for the scattering amplitude in the limit of infinite cut-off radius. The connection to the standard Coulomb scattering amplitude $A_C(\theta)$ turned out, however, to be different from the standard form used widely in the literature and is given in (24). Our form consists of two terms, one of which is the standard one, $e^{-2i\eta \ln 2pR} A_C(\theta)$. To that, however, is added a new expression which is singular at $\theta = 0$ and $\theta = \pi$. These analytical results are fully supported by accompanying numerical investigations. Our renormalization factor for the on-shell t-matrix brings in a very good agreement between the strongly deviating and oscillating numerical solution of the Lippmann-Schwinger equation with the sharp cut off Coulomb potential and the exact Coulomb amplitude. The standard renormalization factor fails completely.

We found also analytically the screening limit of the three-dimensional half-shell t-matrix for the same poten-

tial. Numerical solutions of the three-dimensional Lippmann-Schwinger equation for large cut-off radii agree fairly well with the asymptotic values.

Acknowledgments

This work was supported by the Polish 2008-2011 science funds as the research project No. N N202 077435. It was also partially supported by the Helmholtz Association through funds provided to the virtual institute ‘‘Spin and strong QCD’’ (VH-VI-231) and by the European Community-Research Infrastructure Integrating Activity ‘‘Study of Strongly Interacting Matter’’ (acronym HadronPhysics2, Grant Agreement n. 227431) under the Seventh Framework Programme of EU. The numerical calculations have been performed on the supercomputer cluster of the JSC, Jülich, Germany.

References

1. J.R. Taylor, *Nuovo Cimento* **B23**, (1974) 313.
2. M.D. Semon and J.R. Taylor, *Nuovo Cimento* **A26**, (1975) 48.
3. E.O. Alt, W. Sandhas, and H. Ziegelmann, *Phys. Rev.* **C17**, (1978) 1981.

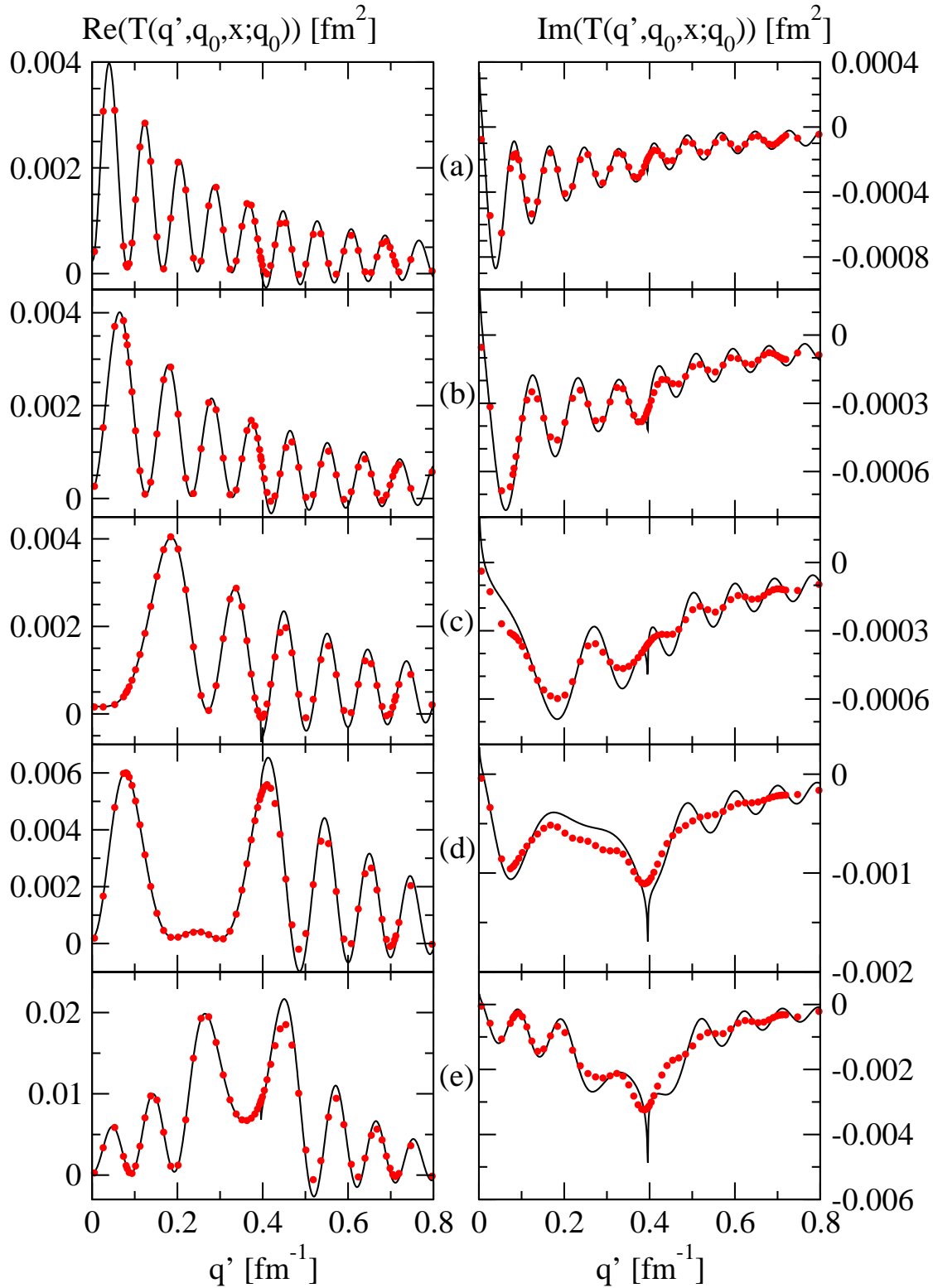


Fig. 3. (color online) The real (left) and imaginary (right) part of the half-shell t-matrix $T(q', q_0, x; q_0)$ for the sharply cut-off Coulomb potential with the cut-off radius $R = 80$ fm. The solid (black) line represents the asymptotic analytical expression given in (34) and (37). The (red) dots show our numerical results. From top to bottom five different values of x are chosen: (a) $x = -0.91$, (b) $x = -0.50$, (c) $x = 0.03$, (d) $x = 0.62$, (e) $x = 0.90$.

4. V.G. Gorshkov, Sov. Phys. - JETP **13**, (1961) 1037.
5. V.G. Gorshkov, Sov. Phys. - JETP **20**, (1965) 234.

6. W.F. Ford, Phys. Rev. **133**, (1964) B1616.
7. W.F. Ford, J. Math. Phys. **7**, (1966) 626.

8. W. Glöckle, J. Golak, R. Skibiński, and H. Witała, *Phys. Rev.* **C79**, (2009) 054008.
9. W. Glöckle, J. Golak, R. Skibiński, and H. Witała, *Few-Body Systems*, DOI 10.1007/s00601-009-0058-z.
10. Y.V. Popov, K.A. Kouzakov, V.L. Shablov, arXiv:0908.3137.
11. L.P. Kok, H. van Haeringen, *Phys. Rev. Lett.* **46**, (1981) 1257.
12. Ch. Elster, J.H. Thomas, and W. Glöckle, *Few-Body Systems* **24**, (1998) 55.
13. E.O. Alt, A.M. Mukhamedzhanov, M. M. Nishonov, and A. I. Sattarov, *Phys. Rev.* **C65**, (2002) 064613.
14. A. Deltuva, A. C. Fonseca, and P. U. Sauer, *Phys. Rev.* **C71**, (2005) 054005.